Available online at www.sciencedirect.com
SCIENCE DIRECT®
International Journal of Heat and Mass Transfer 48 (2005) 5284–5296
International Journal of HEAT and MASS TRANSFER
www.elsevier.com/locate/ijhmt

Scaling heat transfer in fully developed turbulent channel flow

Tie Wei [a], Paul Fife [c,*], Joseph Klewicki [b], Patrick McMurtry [b]

[a] Department of Mechanical Engineering, Penn State University, United States
[b] Department of Mechanical Engineering, University of New Hampshire, United States
[c] Department of Mathematics, University of Utah, Salt Lake City, UT 84112, United States

Received 2 December 2004; received in revised form 20 July 2005
Available online 3 October 2005

Abstract

An analysis is given for fully developed thermal transport through a wall-bounded turbulent fluid flow with constant heat flux supplied at the boundary. The analysis proceeds from the averaged heat equation and utilizes, as principal tools, various scaling considerations. The paper first provides an accounting of the relative dominance of the three terms in that averaged equation, based on existing DNS data. The results show a clear decomposition of the turbulent layer into zones, each with its characteristic transport mechanisms. There follows a theoretical treatment based on the concept of a scaling patch that justifies and greatly extends these empirical results. The primary hypothesis in this development is the monotone and limiting Peclet number dependence (at fixed Reynolds number) of the difference between the specially scaled centerline and wall temperatures. This fact is well corroborated by DNS data. A fairly complete qualitative and order-of-magnitude quantitative picture emerges for a complete range in Peclet numbers. It agrees with known empirical information. In a manner similar to previous analyses of turbulent fluid flow in a channel, conditions for the existence or nonexistence of logarithmic-like mean temperature profiles are established. Throughout the paper, the classical arguments based on an assumed overlapping of regions where the inner and outer scalings are valid are avoided.

Keywords: Turbulence; Heat transfer; Scaling patches; Scaling; Channel flow; Peclet number

1. Introduction

Convective heat transfer from surfaces beneath a flowing fluid impact a large number of technologically important applications [1,2]. Of course, if the flow is turbulent, the rate of this heat transfer is significantly augmented relative to the laminar flow condition [2]. A substantial body of evidence [3] points to important connections between the mechanisms for this enhanced rate of heat transfer and those affecting momentum transport that, for example, also underlie the enhanced surface shear stress in such flows. These connections between momentum and heat transport provide a level of justification for the popular analogy-based correlations often employed in practical engineering computation strategies, e.g., [1,2]. At perhaps an even more pervasive level,

* Corresponding author. Tel.: +1 801 364 3281; fax: +1 801 581 4148.
E-mail address: fife@math.utah.edu (P. Fife).

0017-9310/$ - see front matter © 2005 Elsevier Ltd. All rights reserved.
doi:10.1016/j.ijheatmasstransfer.2005.07.035

Nomenclature

Q_w	wall heat flux
u_τ	friction velocity
Pr	Prandtl number, $Pr = \frac{\nu}{\alpha}$
U^+	inner normalized mean streamwise velocity, $U^+ = \frac{U}{u_\tau}$
$r(\eta)$	normalized mean velocity, $r(\eta) = \frac{U}{U_B}$
$r_\sigma(\eta)$	rescaled r, see following (17)
Pe_τ	Peclet number, $Pe_\tau = Pr\,Re_\tau$
Re_τ	Reynolds number, $Re_\tau = \frac{\delta u_\tau}{\nu} = \delta^+$
L^θ_β	hierarchy of layers
T	inner normalized turbulent thermal flux, $T = \langle v^+ \frac{\theta}{\theta_\tau} \rangle$
T^β	adjusted turbulent thermal flux, defined in Eq. (22)
T^β_m	peak value of T^β
y^+	inner normalized distance from wall, $y^+ = \frac{y u_\tau}{\nu}$
y_σ	new inner normalized distance, $y_\sigma = \frac{\eta}{\sigma^2}$
$y_{\sigma m}(\beta)$	location of T^β_m
β	a small number, introduced in (22)
Θ^+	inner normalized mean temperature
Ψ	renormalized temperature, $\Psi = \frac{\Phi}{\sigma^2}$
η	outer normalized distance, $\eta = \frac{y}{\delta}$
σ^2	maximum value of Φ
α	molecular thermal diffusivity
δ	channel half height
θ_τ	friction temperature
ρ_m	mass density
Θ_w	wall temperature
Φ	normalized mean temperature, $\Phi = \frac{\Theta_w - \Theta}{Pe_\tau \theta_\tau}$
Φ_c	centerline value of Φ
ϵ	small number in the momentum field analysis, $\epsilon^2 = \frac{1}{\delta^+}$
$^+$	quantities normalized by τ_w, Q_w, ρ and ν
$_m$	maximum location or value
$\hat{}$	mesoscaling and hierarchy scaling, e.g., $\widehat{T}$: mesoscaled turbulent thermal heat flux

these connections also often constitute part or all of the conceptual framework for describing the physics of turbulent heat transfer.

Somewhat contrary to such notions, however, is the considerable body of evidence indicating that turbulent scalar fields can exhibit behaviors distinct and neither intuitively connected nor rationally predictable from an understanding of the momentum field alone [4]. Relative to general heat transfer prediction, these observations would seem to indicate that momentum and scalar transport are more tenuously (or at least more subtly) related than the popular analogies might lead one to believe. One of the present objectives is to more clearly elucidate the relative importance of the underlying mechanisms for turbulent heat transfer near walls, their scaling behaviors and their connections to the fluid dynamical mechanisms.

The most common point of departure for addressing the problem of turbulent heat transfer near walls involves simultaneous consideration of the appropriately simplified, once-integrated, time averaged, differential equations describing the conservation of linear momentum and thermal energy, e.g., [2,5]. Of course, the process of time averaging yields the classical closure problem(s) in which the momentum and energy equations are indeterminate owing to the presence of the kinematic Reynolds shear stress, $\langle uv \rangle$, and turbulent heat flux (to be more accurate, turbulent temperature flux), $\langle v\theta \rangle$, respectively. Attempts to close these equations have invoked various phenomenological models [3,6,7]. Regarding the efficacy of such approaches, the recent efforts of Churchill and his co-workers [8–10] are particularly noteworthy. In these studies they invoke a novel local normalization of the Reynolds shear stress and turbulent heat flux. Significantly, consideration of the aforementioned, once-integrated, forms of momentum and energy equations reveals rigorously defined functions for the eddy viscosity, mixing length and turbulent Prandtl number in terms of these locally normalized functions. Furthermore, Churchill et al. show that normalization of the local turbulent heat flux by the total local heat flux (or similarly, the Reynolds stress by the total shear stress) leads to an attractive framework for constructing accurate correlating equations (i.e., curve fits) having considerable applied utility.

Owing to their implicit, and sometimes explicit, empiricism, however, these and other similar methodologies do not optimally serve the present objectives, since, for example, the connections between the functional form of any given correlating equation and the true scaling behaviors describing the underlying transport mechanisms are not rigorously established. Perhaps even more significantly, these (and most other approaches) begin with the once-integrated form of the equations. Through an analysis of the actual mean momentum balance (the terms of which comprise stress gradients rather than stresses), Wei et al. [11] have revealed an alternative physical/theoretical framework for describing the structure of wall-bounded flows. This framework includes a structure for such flows that differs considerably from the nearly universally accepted sub-, buffer, logarithmic and wake layer structure. In doing so, it also, for

example, unambiguously reveals that viscous forces affect dynamics much farther into the flow from the wall than previously believed. Furthermore, this framework has provided the impetus for follow-on studies [12–15] that explore in detail many scaling considerations and implications for physical models. More broadly, these efforts clarify that the physical/mathematical interpretations of the unintegrated form of the mean momentum balance are directly associated with the mechanisms describing the time rate of change of mean momentum; while the first integral of this equation has a distinctly different interpretation, describing the mechanisms associated with the contributions to the flux of momentum.

The present study initiates the analogous exploration of the fundamental behaviors of turbulent heat transfer in wall-bounded flows by following the same strategy employed by Wei et al. [11] and subsequent papers in their study of mean flow dynamics. Specifically, the present effort begins by using available high resolution data to examine the behavior by which the unintegrated form of the mean energy equation is balanced. From this the physical layer structure of the thermal energy field is found. Further multiscale studies, based on the concept of scaling patches, are pursued with the object of constructing a picture of its scaling behaviors relative to variations in Reynolds number and/or Peclet number.

In contrast, it is relevant to reiterate that past theoretical approaches to turbulent heat transfer have largely been based on hypotheses designed to close the Reynolds averaged equation for the mean velocity and mean temperature, or on dimensional considerations. As stated by Perry and Schofield, "*The physical basis of the closing hypotheses is of limited soundness, and the ultimate success of this approach seems doubtful.*" [16]. Therefore it is rational to try another approach and to ascertain the scaling behaviors of turbulent heat transfer as revealed solely by an analysis of the equations. Of course, it should not be expected that these arguments alone will yield a complete solution of the problem. However, recent studies [11–15] of the averaged momentum equation in analogous contexts show that scaling properties and much flow physics can be found through such methodologies.

Section 2 is devoted to deriving and explaining the basic averaged heat equation and boundary conditions employed in the paper for fully developed heat transport. Especially noteworthy is the non-traditional temperature unit (7) found to be appropriate. The flow is shown in Section 3 to be partitioned into four zones according to the relative dominance of the three heat transport terms in the basic energy balance equation derived in Section 2. An extensive multiscale analysis of the scaled heat equation is begun in Section 4. This analysis reveals strong Peclet number, Pe_τ, dependencies. When $Pe_\tau \ll 1$, there is only one appropriate scaling of the variables. In particular, distance from the wall is scaled by the usual outer scaling, even near the wall, and temperature is measured by the new unit just mentioned. When $Pe_\tau \gg 1$, however, the magnitude of the centerline scaled temperature, relative to the wall temperature, serves as the proper small parameter with which to build asymptotics for inner, outer, and mesolayers. The magnitude of this temperature scale depends monotonically on Pe_τ, for fixed Reynolds number. Previous analysis of the flow structure of turbulent channel flow provides a paradigm for this construction. Finally Section 5 is devoted to extending that paradigm to account for a continuum of scaling patches, in addition to the three already studied, which altogether cover a good part of the channel cross-section. It is in Section 5 that the relevance of this continuum of layers to the question of the logarithmic nature of the mean temperature profile is brought to light.

2. Statement of the problem

2.1. The heat equation

A detailed derivation of the heat transfer equation for turbulent wall bounded flows appears, for example, in the books by Monin and Yaglom [5], Landau and Lifshitz [17] and Kays and Crawford [2]. Since the present paper relies heavily on the analysis of the mean heat equation, it is appropriate to sketch the derivation briefly. For incompressible flow with constant properties and with the heat transfer effect of viscous dissipation neglected, the instantaneous energy equation is given by

$$\frac{\partial\tilde{\theta}}{\partial\tau}+\tilde{u}_j\frac{\partial\tilde{\theta}}{\partial x_j}=\alpha\frac{\partial^2\tilde{\theta}}{\partial x_j\partial x_j}, \tag{1}$$

where $\tilde{\theta}$ and $\tilde{u}_j$ are the instantaneous temperature and velocity, τ is time, and α is the molecular thermal diffusivity. The dimensions of α are the same as those of the kinematic molecular viscosity ν, $[\frac{L^2}{\tau}]$. The Prandtl number is defined by the ratio, $Pr=\frac{\nu}{\alpha}$. The heat equation has a form very similar to that of the momentum equation, except there is no pressure term in the former.

To obtain the averaged heat equation, one decomposes the variables $\tilde{\theta}=\Theta+\theta$; $\tilde{u}_j=U_j+u_j$ into mean and fluctuating parts and takes the average of (1); see e.g. [5]. Specializing to 2D steady channel flow with coordinates (x,y) and fluctuation velocity components (u,v) gives

$$U\frac{\partial\Theta}{\partial x}=\alpha\frac{\partial^2\Theta}{\partial y^2}-\frac{\partial\langle v\theta\rangle}{\partial y}. \tag{2}$$

Traditionally the friction temperature (Kader et al. [3] called it the heat flux temperature) is defined by $\theta_\tau=\frac{Q_w}{(\rho_m C_p)u_\tau}$, where $Q_w=-k\frac{\partial\Theta}{\partial y}\Big|_w$ is the heat flux at the wall, $u_\tau=\sqrt{\tau_w/\rho_m}$ is the fluid flow friction velocity, τ_w

is the wall shear stress, ρ_m is the mass density, and C_p is the specific heat. The molecular thermal conductivity, k, is related to α by $\alpha = \frac{k}{\rho_m C_p}$. The wall Reynolds number, Re_τ, which is the same as the inner normalized channel half-width $\delta^+ = \frac{u_\tau}{\nu}\delta$, will play an important role in the following analysis. The same will be true of the wall Peclet number

$$Pe_\tau = Pr\,\delta^+. \tag{3}$$

It will always be assumed that $Re_\tau = \delta^+ \gg 1$.

The prescribed heat flux at $y = 0$ results in the boundary condition,

$$\frac{Q_w}{\rho_m C_p} = -\alpha \left.\frac{\partial \Theta}{\partial y}\right|_w. \tag{4}$$

2.2. The fully developed state

Fully developed heat transfer, governed by (2) with constant heat flux Q_w prescribed at the wall $y = 0$ for $x > 0$, is approached at positions sufficiently far downstream, i.e. for large values of x. This state is characterized by the x-derivative of the temperature being a positive constant, independent of both x and position in the channel. It is analogous to steady fully developed turbulent Poiseuille flow through a channel, wherein the x-derivatives of all averaged quantities are 0. The value of the constant in the present case can be determined by applying an energy balance to a section of the channel. It turns out to be $\frac{u_\tau \theta_\tau}{\delta U_B}$, where $U_B = \frac{1}{\delta}\int_0^\delta U(y)\,dy$ is the bulk mean velocity. Thus, in thermally fully developed flow, the temperature is a linearly increasing function of x (therefore unbounded), with the rate of increase given by $\frac{u_\tau \theta_\tau}{\delta U_B}$, i.e., $\frac{\partial \Theta}{\partial x} = \frac{\partial \Theta_w}{\partial x} = \frac{u_\tau \theta_\tau}{\delta U_B}$, for each x and y, where Θ_w is the temperature at the location on the wall with the same value of x. The temperature and turbulent heat flux profiles under fully developed conditions will be of primary concern.

2.3. Normalizations

Conventionally the velocity, length, and temperature units u_τ, $\frac{\nu}{u_\tau}$ and θ_τ are used to normalize the averaged heat equation. This results in the usual inner-normalized mean velocity $U^+ = \frac{U}{u_\tau}$ and distance $y^+ = \frac{y}{\nu/u_\tau}$ from the wall. The usual inner normalized heat equation derived from (2) is,

$$0 = -\frac{1}{\delta^+}\frac{U^+}{U_B^+} + \frac{1}{Pr}\frac{\partial^2 \Theta^+}{\partial y^{+2}} + \frac{\partial(-\langle v^+\theta^+\rangle)}{\partial y^+}. \tag{5}$$

Similarly, using the channel half height δ to normalize the distance, $\eta = \frac{y}{\delta}$, one obtains the usual outer normalized heat equation:

$$0 = -\frac{U^+}{U_B^+} + \frac{1}{Pr\,\delta^+}\frac{\partial^2 \Theta^+}{\partial \eta^2} + \frac{\partial(-\langle v^+\theta^+\rangle)}{\partial \eta}. \tag{6}$$

A considerably more revealing alternative, however, is to use the units u_τ, δ, and $\theta_\tau Pe_\tau = \theta_\tau \delta^+ Pr$. This choice recovers the same inner velocity and outer normalized distance η, but a new temperature variable Φ, which will be referenced to the wall temperature, Θ_w in order to more accurately incorporate the thermally fully developed condition. In all, the new variables (U^+, η, Φ) are defined by

$$U = u_\tau U^+, \quad y = \delta\eta = \frac{\nu\delta^+}{u_\tau}\eta,$$
$$\Phi = \frac{\Theta_w - \Theta}{\delta^+ Pr\,\theta_\tau} = \frac{\Theta_w - \Theta}{Pe_\tau\,\theta_\tau}. \tag{7}$$

This locally defined temperature renders a self-preserving form for the temperature field. Let $T = \langle v^+ \frac{\theta}{\theta_\tau}\rangle$ (in this expression, temperature is scaled differently than in (7)). The fully developed condition implies no x-dependence, so the variables Φ and T (see below) will depend only on η. The result is

$$\frac{d^2\Phi}{d\eta^2} + \frac{dT}{d\eta} + r(\eta) = 0, \tag{8}$$

where $r(\eta) = \frac{U(\eta)}{U_B}$.

The function $r(\eta)$, being a scaled mean velocity profile, also depends on δ^+; that dependence will not be displayed, because it plays a minor role in the following development. This function is O(1) for all values of η except in a thin turbulent wall layer. This property will be important in what follows. Eq. (8) could be called an outer normalized equation of heat transport; it differs from the traditional outer formulation (6) and will be our basic thermal energy balance equation for the thermal transport problem.

Boundary conditions at $\eta = 0$ are

$$\Phi = 0, \quad \frac{d\Phi}{d\eta} = 1, \quad T = \frac{dT}{d\eta} = 0. \tag{9}$$

At the centerline $\eta = 1$,

$$T = 0, \quad \frac{d\Phi}{d\eta} = 0. \tag{10}$$

The second condition in (9) is the form that (4) takes in the present units. The conditions (9) and (10) are not boundary conditions in the usual sense of stipulations which lead to a unique solution of some boundary value problem. Rather (8), even under these conditions, is underdetermined (one equation with two unknowns), with no unique mathematical solution. The object here, since there does exist a unique unknown physical solution, is to deduce important scaling properties that that solution has.

Note that neither Eq. (8) nor the boundary conditions (9) and (10) depend overtly on any parameter except δ^+, and that dependence (through the function r) will be of little consequence. However, while each of the terms in (8) is formally O(1), there is no reason to

expect that that is their actual magnitude, except for the last term $r(\eta)$, which is known to remain O(1) except in the wall layer. Despite no explicit occurrence on Pe_τ in (8), that parameter is embedded therein; the variables generally will depend on it, but in such a way that the differential equation is satisfied identically. The present task will be to try to make that hidden dependence explicit, by means of further rescaling.

2.4. Comparison of momentum transfer and scalar transfer

Thermal transfer and momentum transfer are closely related, with Θ^+ analogous to U^+, Q_w to τ_w, and various other analogies among the parameters of the two problems. In this context, it is relevant to point out that in engineering applications the 'Reynolds analogy' is quite often used when $Pr = O(1)$. (Its deficiencies, at least for other values of Pr, will be brought out in the current paper.) Under the Reynolds analogy, in view of the similarity of the basic equations, the temperature profile is assumed to be the same as that of the velocity profile; in particular, $\frac{\Theta_w-\Theta_c}{\theta_\tau} = U_c^+$.

3. Principal layer structure

For comparative purposes, this section first briefly reviews the traditional layer structure for developed wall-bounded turbulent heat transfer. The physical layer structure as prescribed by the relative magnitude of the terms in (8) is then presented.

3.1. Established picture

The thermal wall layer for turbulent flow is traditionally divided into four layers: the molecular transport sublayer, the buffer layer, the logarithmic layer, and the outer layer, with the same physical reasoning as for the momentum wall layer [3,6]. The following facts are noted: (i) In addition to the Reynolds number, the thermal equations involve another parameter, Pe_τ, which makes the thermal case more complicated, (ii) The extent of the 'thermal buffer layer' is not as clear as that of the 'momentum buffer layer', (iii) Kader provides Pr-dependent coefficients for the logarithmic layer based mainly on fitting to the experimental data [6].

3.2. Revised principal layer structure

The present methodology ascertains an alternative physical layer structure directly from the properties of the terms appearing in the governing equation. There are three terms in the mean heat equation (8), relating to the production of heat due to molecular diffusion transport, turbulent transport, and streamwise mean

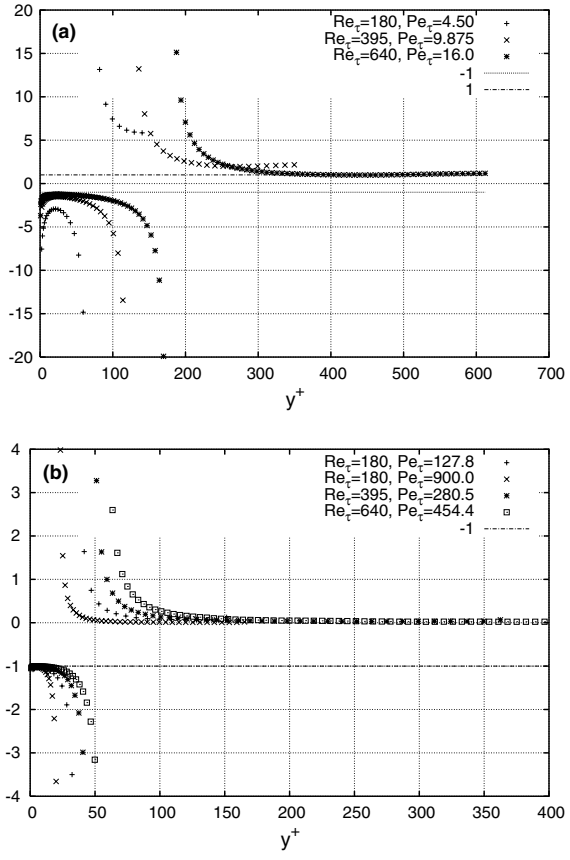

Fig. 1. Heat flux gradient ratio, $(d^2\Phi/d\eta^2)/(dT/d\eta)$. (a) Low Pe_τ. (b) $Pe_\tau \gg O(1)$. DNS data from Kawamura's group [18] and Kasagi's group [19].

advection (the former two are gradients of the respective fluxes). These terms sum to zero to reflect energy conservation. To estimate the relative magnitude of the terms, Fig. 1 provides the ratio of the gradient of the molecular diffusion flux to that of the turbulent transport flux:

$$\frac{\alpha \dfrac{d^2\Theta}{dy^2}}{-\dfrac{d\langle v\theta\rangle}{dy}} = \frac{\dfrac{d^2\Phi}{d\eta^2}}{\dfrac{dT}{d\eta}}.$$

(1) Small or moderate Pe_τ: As shown in Fig. 1(a), for low Peclet number, the magnitude of the molecular diffusion term $|\frac{d^2\Phi}{d\eta^2}|$ is always larger than that of the turbulent term $|\frac{dT}{d\eta}|$. It is especially worth noting that the molecular heat transport is larger than the turbulent heat transport in the 'outer region' where the flow is inertially dominated. Note also that $\frac{d\Phi}{d\eta}$ is larger than the turbulent heat flux, T, across the whole layer for low Pe_τ (Fig. 2). This situation is quite distinct from the momentum equation. For the momentum field, the diffusive and turbulent contributions to the time rate of change of momentum balance each other, out to a position near

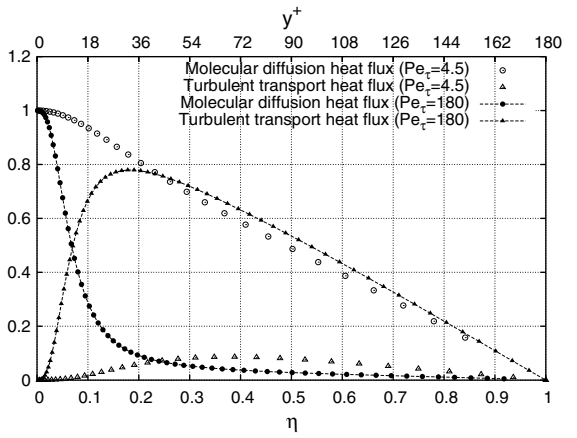

Fig. 2. The molecular diffusion heat flux $\frac{d\Phi}{d\eta}$ and turbulent heat flux, $T = \langle v^+ \frac{\theta}{\theta_\tau} \rangle$ for two Peclet numbers: in one case $Pe_\tau = O(1)$ and in the other, $Pe_\tau = 180$. Note that for $Pr = O(1)$ and not too high Reynolds number (i.e., $Re_\tau = 180$), $\frac{d\Phi}{d\eta}$ is always larger than T. Same source of DNS data as in Fig. 1.

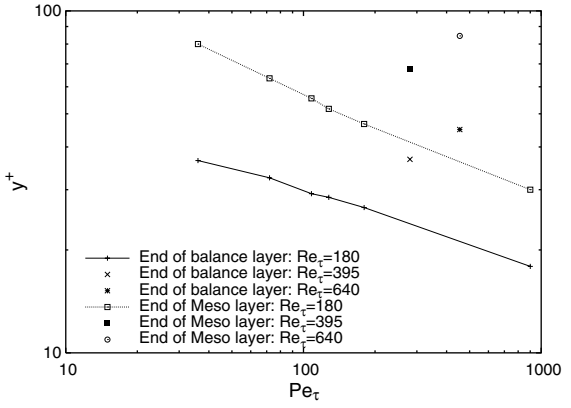

Fig. 3. The inner normalized extent of the layers in fully developed thermal channel flow. It is plotted as $\delta^+\eta$ and $Pe_\tau = Re_\tau * Pr$.

the peak in the Reynolds shear stress, while the turbulent stress dominates the viscous stress beyond the buffer layer. Therefore, for low Peclet number, the Reynolds analogy is incongruous with the behavior of the terms in the governing equation. For low Prandtl number, however, as Reynolds number increases (see Fig. 1(a), the case when $Re_\tau = 640$ and $Pr = 0.025$), the ratio plotted approaches -1 in a certain region near the surface.

(2) Moderate or large Pe_τ: As shown in Fig. 1(b), there is a clear -1 ratio region. This -1 ratio region grows outward with increasing Reynolds number, and it moves inward with increasing Prandtl number. The reasons for this are explained later in Section 4.4.

The behavior of the ratio of the two heat flux gradient terms, as shown in Fig. 1(a) and (b) indicate the following layer structure for Pe_τ moderate or large:

- *Layer I:* Molecular diffusion/mean advection balance layer, where the molecular diffusion terms balance the mean advection term, while the turbulence term is not important. (Note that this sublayer is clearer for low Pe_τ data, as shown in Fig. 1(a).)
- *Layer II:* Heat flux gradient balance layer, where the heat equation balance is essentially between the molecular diffusion term and the turbulent transport term (aforementioned -1 ratio layer).
- *Layer III:* Mesolayer, where all three terms are important for the heat equation balance (except very close to the peak value of T, where the turbulent flux gradient crosses through zero and is negligible).
- *Layer IV:* Inertial layer where the heat equation balance is between the mean advection and the turbulent transport term, while the molecular diffusion term is negligible.

3.3. Layer extents

The physical extents of the thermal layer structure shown in Fig. 3 are defined in a way similar to that for the momentum layer structure [11], i.e., the end of the gradient balance layer is defined as $\left(\alpha \frac{d^2\Theta}{dy^2}\right) / \left(-\frac{d\langle v\theta\rangle}{dy}\right) = -2$, and the end of the mesolayer is defined as $\left(\alpha \frac{d^2\Theta}{dy^2}\right) / \left(-\frac{d\langle v\theta\rangle}{dy}\right) = 0.5$. The curves in Fig. 3 are based on the DNS data of Kawamura's group[1] [18] and Kasagi's group[2] [19]. Due to the narrow range of the Reynolds numbers ($Re_\tau = \delta^+ = 180$, 395, 640), and the range of Prandtl number ($0.025 < Pr < 5$), these data, although suggestive, are inconclusive with regard to asymptotic behavior. In Fig. 3, the layer extents are quantified, in inner normalized distance, $y^+ = \delta^+\eta$, to their upper boundaries and are plotted against Pe_τ. The data are for fixed Reynolds number (there are three Reynolds number curves) , so Fig. 3 shows that as Pr increases (or Pe_τ increases in this case), layer II and layer III move towards the wall.

4. Multiscale analysis

4.1. Goals, strategies, and observations

A "scaling patch" is a specified scaling of the variables η and T (see (8)) together with an interval of η-values in which that scaling is natural (see [12,13]). The object of the following analysis is to explain and develop

[1] http://murasun.me.noda.tus.ac.jp/db/dns.
[2] http://www.thtlab.t.u-tokyo.ac.jp/DNS/.

an approach to the determination of the structure of the Φ and T profiles, based on the concept of scaling patches. This is shown to be analogous to the analysis in [12,13,11] of U^+ and T profile structures for steady turbulent (Couette and Poiseuille) flow through a channel. This correlates in part with the results described in Section 3, especially in regard to the mesolayer, which will be found to have its own "mesoscaling".

The strategy will be first to begin with the scaled form (8)–(10) of the averaged differential energy balance and boundary conditions. Under the normalization employed, all three terms of the differential equation have nominal order O(1) and neither the differential equation nor boundary conditions have any explicit parameter dependence. Eq. (8) is similar in form to that which occurs in the study of steady turbulent flow in a channel. In fact, many of the tools used in the latter analysis find application in the former as well. However, the thermal problem has one extra parameter, Pr, in addition to δ^+. This, it turns out, makes for an additional degree of indeterminacy and difficulty.

Next, recognizing that the nominal order of a term does not necessarily correspond to its actual order of magnitude, a rescaling of the variables is undertaken such that after terms of nominal order $\ll 1$ in the resulting differential equation and boundary conditions are discarded, the nominal order of each term in some part of the channel (i.e., some scaling patch) coincides with its actual order of magnitude. Because of the underdetermined nature of the problem, this may involve some examination of empirical data concerning the actual magnitudes of terms. Data indicate that with the possible exclusion of a thin wall layer, the ratio of the molecular diffusion heat flux gradient to the turbulent heat flux gradient (ratio of the first to the second term in (8)) depends strongly on Pe_τ, even though Pe_τ is not explicit in the energy balance Eq. (8). The analysis is based on this property (as reflected in the hypothesis stated below) as well as the supposition that the ratio is very large when $Pe_\tau \ll 1$, and except in a wall layer, is very small when $Pe_\tau \gg 1$.

This approach allows construction of scaling patches and deduction of the qualitative structure of the temperature and turbulent thermal flux profiles.

4.2. Dependence of Φ and T on Pe_τ

Before making hypotheses, it is useful to examine the properties of Φ with DNS data. The Reynolds number and Peclet (or Prandtl) number dependencies of Φ are shown in Fig. 4. The dependencies of T on those two numbers are shown in Fig. 5. The centerline values, Φ_c, of Φ for different Peclet numbers are shown in Fig. 6(a). All of these data show a general monotone decrease of Φ as Pe_τ increases, $\delta^+ = Re_\tau$ being held constant. This same trend, for the respective η-derivatives

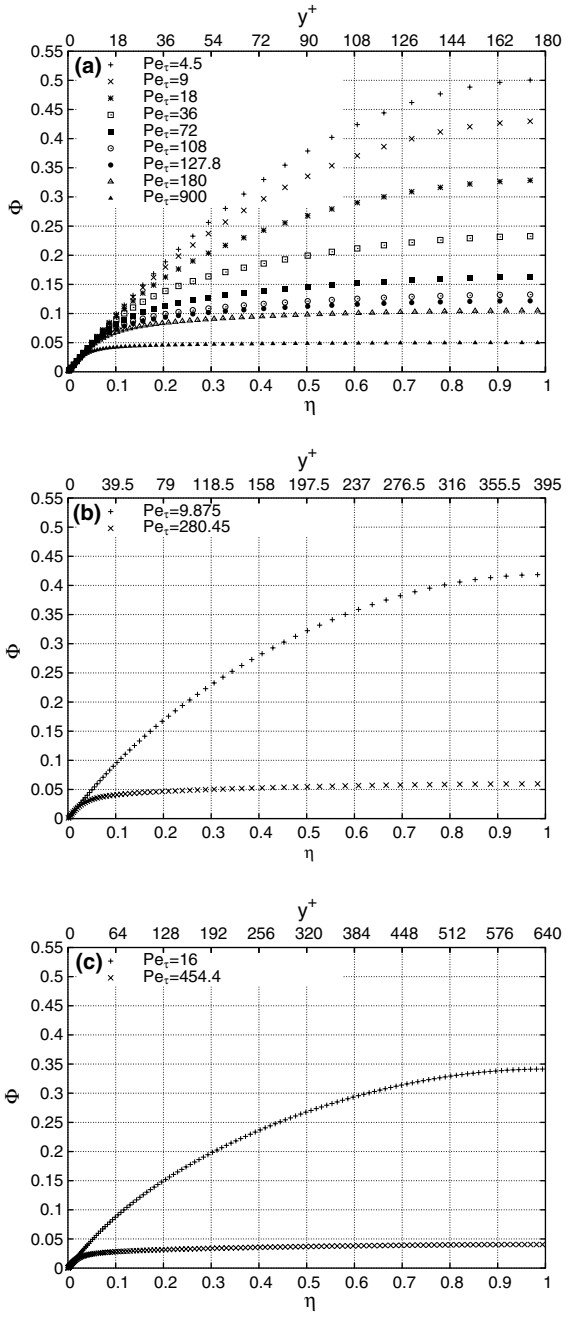

Fig. 4. The Φ profiles across the half channel for different Reynolds numbers and different Peclet numbers. (a) Fixed Reynolds number $Re_\tau = 180$. (b) $Re_\tau = 395$. (c) $Re_\tau = 640$. The DNS data are from Kawamura's group.

of Φ, can be seen in Fig. 2. In the case of the second derivatives, if one restricts attention to the outer region in layer IV, the plots in Fig. 1 serve, to some extent, to indicate the same monotone trend, because the numera-

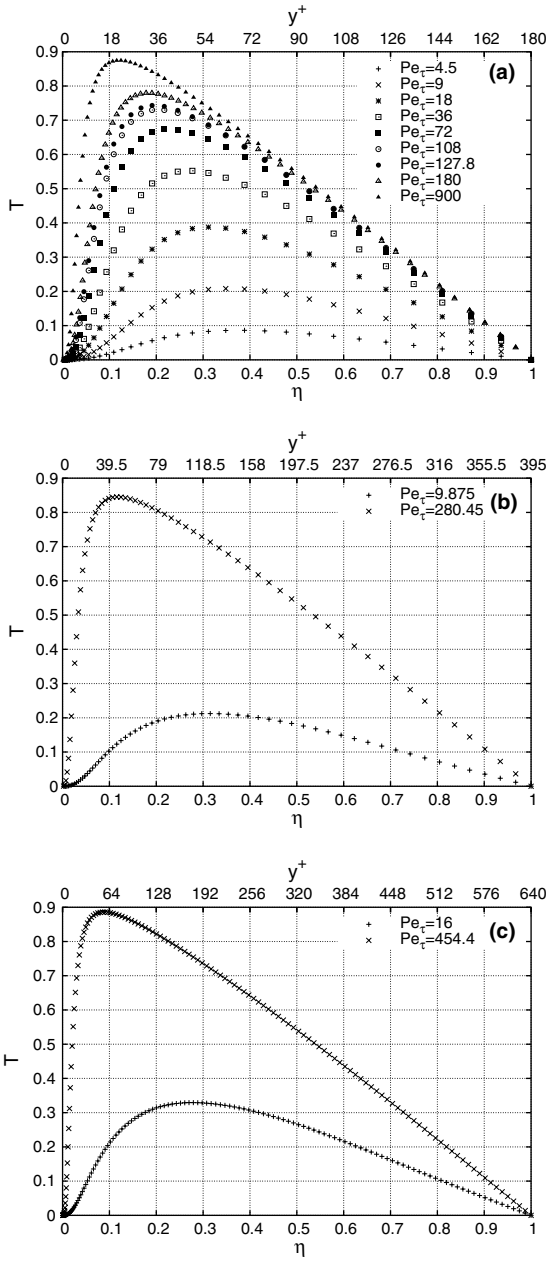

Fig. 5. Turbulent heat flux, T, profiles across the half channel for different Reynolds numbers and different Peclet numbers. (a) Fixed Reynolds number of $Re_\tau = 180$. (b) $Re_\tau = 395$. (c) $Re_\tau = 640$. The DNS data are from Kawamura's group.

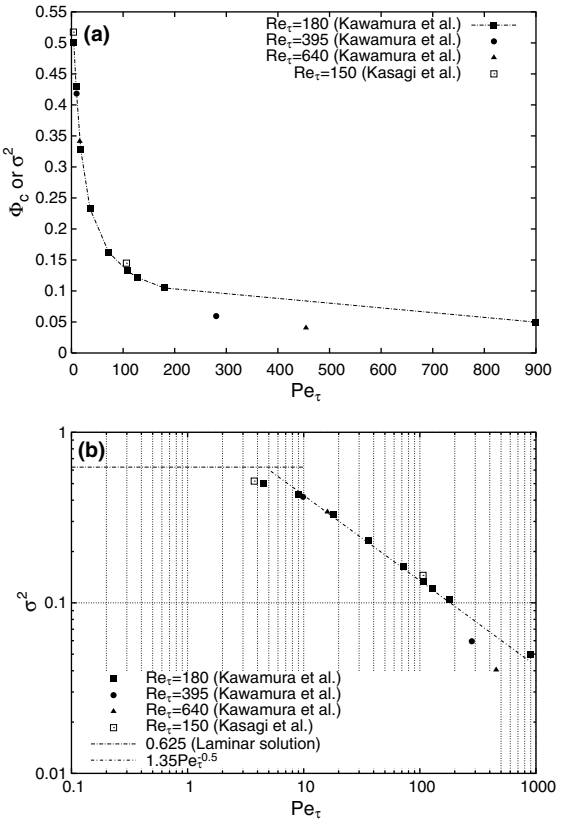

Fig. 6. The dependence of centerline Φ values, Φ_c, on Peclet number $Pe_\tau = Re_\tau Pr$. (a) Φ_c versus Pe_τ on linear axes. (b) Φ_c versus Pe_τ on log axes. The data suggest a power law dependence with exponent ~ -0.5. The DNS data are from Kawamura's group. The Reynolds number of the data are $Re_\tau = 180$, 395, 640. The Peclet numbers are between $Pe_\tau = 4.5$ and $Pe_\tau = 900$. Note that σ^2, defined above (15) and occurring on the vertical axes, will be one of the principal parameters of the analysis to follow.

tor of the ratio plotted there is just the second derivative in question, while the denominator is almost constant. The data in Fig. 6 suggest that $\Phi_c \to 0$ as $Pe_\tau \to \infty$ ($Pr \to \infty$), and that Φ_c approaches an O(1) limit as $Pe_\tau \to 0$ ($Pr \to 0$).

It is relevant to note the Pe_τ and Re_τ dependence of the centerline value of the ratio plotted in Fig. 1. Fig. 1(a) shows that this value decreases with increasing Re_τ. Fig. 1(b) shows that when Pe_τ is larger, the ratio is very small, independent of Re_τ. The monotone dependence of Φ and its derivatives upon Pe_τ suggests that when Pe_τ decreases, δ^+ remaining fixed, the second term in (8), $\frac{dT}{d\eta}$, decreases and the first term, $\frac{d^2\Phi}{d\eta^2}$, increases. Of course since the third term in (8) is always O(1) (both nominally and actually), smallness of either of the first two terms implies that the other is O(1). In view of this, the following limiting behaviors are hypothesized:

Hypothesis. For fixed values of δ^+ and η, Φ is a monotonic decreasing function of Pe_τ, approaching 0 as $Pe_\tau \to \infty$ and approaching an O(1) limit as $Pe_\tau \to 0$. The same is true of $\frac{d\Phi}{d\eta}$ and $|\frac{d^2\Phi}{d\eta^2}|$, except that the first limit, namely as $Pe_\tau \to \infty$, is only valid outside a narrow wall layer near $\eta = 0$.

Immediate consequences of these hypothesized behaviors are:

(a) For each fixed large δ^+, when Pe_τ (or Pr) is small enough, the second term in (8) can be neglected, resulting in a well-determined boundary value problem,

$$\frac{d^2\Phi}{d\eta^2} + r(\eta) = 0, \tag{11}$$

$$\Phi(0) = 0, \quad \frac{d\Phi}{d\eta}(0) = 1, \quad \frac{d\Phi}{d\eta}(1) = 0, \tag{12}$$

whose unique solution can be written down, since $\int_0^1 r(\eta)\,d\eta = 1 : \Phi(\eta) = \eta + \int_0^\eta (s-\eta) r(s)\,ds$. This is supported by the DNS data shown in Fig. 7, and is compatible with Fig. 1.

(b) For each fixed large δ^+, when Pe_τ is large enough, the first term in(8) can be neglected, except in a narrow wall layer near $\eta = 0$. Outside the wall layer, there results the approximate equation,

$$\frac{dT}{d\eta} + r(\eta) = 0, \tag{13}$$

$$T(1) = 0, \tag{14}$$

which again has a unique solution.

The existence of an excluded wall layer in case (b) is necessary in order to allow the boundary conditions (9) at the wall to be satisfied. Rescalings will be necessary to reveal the structure of Φ and T in that flow region.

Under the above hypothesis, when Pe_τ is small enough, we have approximate knowledge of the variables Φ and T throughout the channel. Moreover, this is done with a single scaling: the one that produced (8). There is no other scaling needed for different ranges of the variable η. Hence there is only one "scaling patch" [12], and it covers the entire domain.

This is not true when Pe_τ is large, i.e., the case for which there exists a distinct wall layer. This case entails looking for the proper rescaling(s) in that layer. These scalings will depend on Pe_τ as well as on δ^+, both of them large parameters.

The case when Pe_τ is small shows a failure of the Reynolds analogy. The solution has $\Phi = O(1)$, which implies that the analogous inner scaled temperature difference $\Theta_w^+ - \Theta^+ = O(Pe_\tau)$, hence bounded independently of Pe_τ. The analog in turbulent channel flow is the mean velocity U^+, which attains values $\sim C \ln \delta^+$, so it is not bounded.

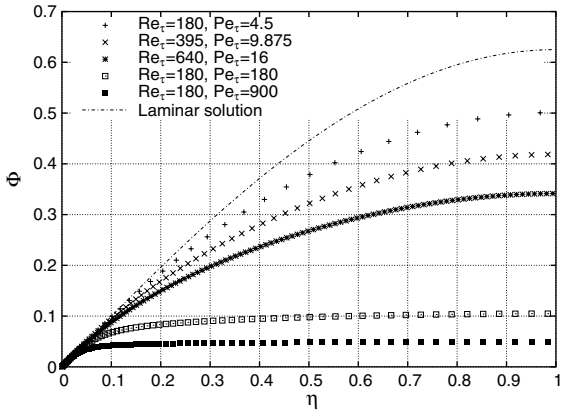

Fig. 7. Φ versus η. The low Pe_τ number temperature profile is close to the laminar temperature profile.

4.3. Scaling framework

The primary unanswered question concerns the structure of the wall layer (case (b) above), especially its dependence on Pe_τ. The approach here will be to build on what is known about the channel flow problem, specifically the framework established in [13,12]. The limiting behaviors hypothesized in the previous section will also be a guiding ingredient. The key to the analysis will be the introduction of a new variable parameter σ, which is directly related to the magnitude of Φ and is indirectly a function of Pe_τ.

Case (a), i.e. (11) and (12) when $Pe_\tau \ll 1$, is not considered because the mean temperature field has no wall layer. The initial focus is on the case when the first term in (8) is small, at least in the outer region.

Define σ by

$$\sigma^2(\delta^+, Pe_\tau) = \max \Phi(\eta) = \Phi(1).$$

Assume now that $\sigma \ll 1$. We define the σ-dependent temperature variable Ψ by,

$$\Phi = \sigma^2 \Psi, \tag{15}$$

so that $\Psi = O(1)$ near the center. This new temperature variable is the same as the non-dimensional commonly employed form $\Psi = (\Theta_w - \Theta)/(\Theta_w - \Theta_c)$. With this, there exists a new outer equation

$$\sigma^2 \frac{d^2\Psi}{d\eta^2} + \frac{dT}{d\eta} + r(\eta) = 0. \tag{16}$$

This equation, with the attendant boundary conditions, is entirely analogous to equations governing turbulent channel flow [11]; in the latter case there is a small parameter ϵ, analogous to σ in (16). We therefore follow the lead of the inner–outer reasoning for [11]. This involves defining a new inner variable y_σ by,

$$y_\sigma = \frac{\eta}{\sigma^2}. \tag{17}$$

This generates a scaled advection function of the inner variable $r_\sigma(y_\sigma) = r(\eta(y_\sigma)) = r(\sigma^2 y_\sigma)$.

From this the following inner form for the energy balance equation is obtained,

$$\frac{d^2\Psi}{dy_\sigma^2} + \frac{dT}{dy_\sigma} + \sigma^2 r_\sigma(y_\sigma) = 0 \tag{18}$$

with boundary conditions $\Psi = T = 0$ at $y_\sigma = 0$, and (from (15), (17) and (12))

$$\frac{d\Psi}{dy_\sigma}(0) = \sigma^{-2}\frac{d\Phi}{dy_\sigma}(0) = \frac{d\Phi}{d\eta}(0) = 1. \tag{19}$$

It would be desirable to quantify what the present formalism predicts regarding how σ depends on δ^+ and Pe_τ (or Pr). For this, the DNS data of Fig. 6 provide guidance.

4.4. The mesoscale and peak location

Eqs. (16) and (18) employ an outer variable η and a σ-dependent inner variable y_σ. As in the momentum field [11], there will be a mesoscaled variable, valid near the maximum of T, defined by

$$\hat{y}_\sigma = \sqrt{y_\sigma \eta} = \frac{\eta}{\sigma}. \tag{20}$$

Analogous to the channel turbulence problem, the location of this maximum is at

$$y_\sigma = y_{\sigma m} = O(\sigma^{-1}), \quad \eta = \eta_m = O(\sigma) \tag{21}$$

(these relations are equivalent to each other).

Fig. 8 clearly corroborates these estimates. In fact, it indicates that η_m is almost a linear function of σ, for at least $Re_\tau = 180$ (there are not enough data points to judge, for the larger values of Re_τ; no doubt any approximate linear relation would have Re_τ-dependent coefficients). Given that the location of the peak value of T, measured in the outer variable η, is an increasing function of σ, the above scaling hypothesis in turn suggests that σ^2, a measure of the magnitude of Φ, increases when Pe_τ decreases (at least for $Pe_\tau \gg 1$). Thus, overall, the peak position as measured in η may be expected to be a decreasing function of Pe_τ. This is strikingly confirmed by DNS simulation results in Fig. 5.

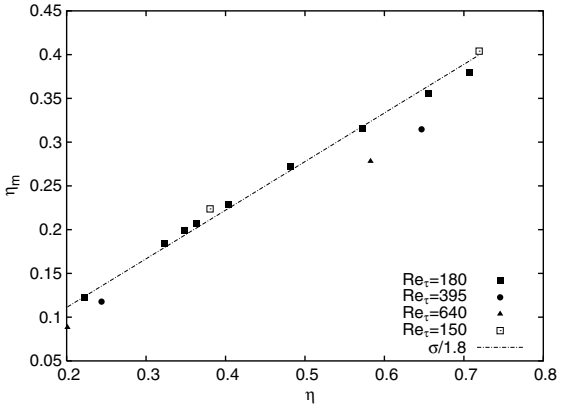

Fig. 8. Maximum T location. Note that the range of $\sigma = (\frac{1}{Pe_\tau}\frac{\Theta_w - \Theta_c}{\theta_\tau})^{0.5}$ is rather limited due to the range of the DNS data.

5. A hierarchy of layers when Pe_τ is moderate or large

The three scalings employed thus far, namely inner, outer, and meso, constitute those appropriate for the scaling patches associated with primary physical layer structure (Fig. 1, Section 3.2). As with the momentum field, however, there is much additional embedded structure. As typified in [12,13], the balance exchange argument leading to a mesolayer centered around the maximum value of T can be generalized to show the existence of a self-similar continuum of scaling patches, one at the peak value of each of a family of adjusted Reynolds stresses: each of which transforms the appropriately scaled energy balance to an invariant form. The same can be done in the present case, since the problem formulation (16) and (19) is highly analogous. The differences are now that (i) the small parameter is σ, whereas in the former case it was ϵ, which had a different physical meaning; and (ii) the convection term $r(\eta)$ is not the constant 1 (although it only deviates significantly from 1 for small η). Structurally, these differences are believed significant since they underlie the precise mechanisms by which analogies between the scaling behaviors for the momentum and temperature fields break down. In what follows, the procedure for showing this self-similar continuum of scales for the temperature field will be explained briefly; especially relevant will be the way of handling the nonconstancy of r.

5.1. The adjusted turbulent thermal fluxes

We proceed from (18), assuming that σ is so small that the graph of $T(\eta)$ has a prominent peak. To dwell somewhat on this issue, the outer approximation is obtained from (13) and (14): $T(\eta) = T_{\text{out}}(\eta) \equiv \int_\eta^1 r(s)\,ds$. From the outer approximation one finds that the function T behaves qualitatively like the Reynolds stress: it rises to achieve a maximum near $T_{\text{out}}(0) = 1(1 - T_{\max} = O(\sigma))$ at a point near the wall satisfying (21), then diminishes monotonically to vanish at the centerline.

To obtain the scale hierarchy, define a family of adjusted turbulent thermal fluxes:

$$T^\beta(y_\sigma) \equiv T(y_\sigma) + \sigma^2 \int_0^{y_\sigma} r_\sigma(s)\,ds - \beta y_\sigma \tag{22}$$

for an interval of values of β to be specified. Inserting this into (18) yields

$$\frac{d^2\Psi}{dy_\sigma^2} + \frac{dT^\beta}{dy_\sigma} + \beta = 0. \tag{23}$$

The next observation is that near a peak value of T^β, the rescaling of (24) below eliminates, in (23), any explicit dependence on β. For a range of values of β, depending somewhat on σ as well as on δ^+, the function $T^\beta(y_\sigma)$ will have a strict local maximum at some point $y_\sigma = y_{\sigma m}(\beta)$,

also depending on Pe_τ and δ^+. As in the channel flow without thermal effects, the existence of a hierarchy of scaling patches, L^θ_β, can be derived, each one centered around $y_{\sigma m}(\beta)$. In the patch, the intrinsic scaling will be given by the following differential transformation from $(\mathrm{d}y_\sigma, \mathrm{d}T^\beta)$ to $(\mathrm{d}\hat{y}, \mathrm{d}\widehat{T})$:

$$\mathrm{d}y_\sigma = \beta^{-1/2}\,\mathrm{d}\hat{y}, \quad \mathrm{d}T^\beta = \beta^{1/2}\,\mathrm{d}\widehat{T}, \quad y_\sigma = y_{\sigma m}(\beta) + \beta^{-1/2}\hat{y},$$
$$T^\beta = T^\beta_m + \beta^{1/2}\widehat{T}, \tag{24}$$

where $T^\beta_m = \max(T^\beta)$. This leads to

$$\frac{\mathrm{d}^2\Psi}{\mathrm{d}\hat{y}^2} + \frac{\mathrm{d}\widehat{T}}{\mathrm{d}\hat{y}} + 1 = 0, \tag{25}$$

which is free of any explicit parameter dependence. Together with the satisfaction of certain conditions that ensure the compatibility of the scaling with known data in a neighborhood of $y_{\sigma m}(\beta)$, this parameter-free equation is sufficient to verify the existence of a scaling patch, L^θ_β, for each β in the range specified. The details are the same as those in [12,13]. The scaling given by (24) is the correct one for the variables y_σ (hence by (17) for η) and T^β in each scaling patch L^θ_β designated by β. However since T, rather than T^β, is the variable of interest, it should be brought out that T will have the same natural scaling in L^θ_β. The details of showing this are the same as in [13,12] and will not be repeated here.

This establishes the continuum of scaling patches; combined with the principal inner-, outer-, and mesopatches, it provides the structural context in which the profiles of Φ and T exist.

5.2. Locations of the $T^\beta(y_\sigma)$

As indicated, the relative locations, in the channel, of the members of the hierarchy of layers, L^θ_β, coincide with the locations of the maxima of T^β. These are not immediately known, because the function T is still unknown. Knowledge of the locations $y_{\sigma m}(\beta)$ provides an important description of the length scales relevant to the heat transfer mechanisms and their dependencies on Pe_τ and δ^+. To get information about the locations $y_{\sigma m}(\beta)$, first set

$$A(\beta) = -\frac{\mathrm{d}^2\widehat{T}}{\mathrm{d}\hat{y}^2}(0) \tag{26}$$

the curvature of the rescaled adjusted turbulent thermal flux profile evaluated at its peak location. This is an O(1) quantity since the scaling used here is the correct one for that location.

Now note from (22) and the fact that $\frac{\mathrm{d}T^\beta}{\mathrm{d}y_\sigma}(y_{\sigma m}) = 0$ (since T^β attains a maximum there)

$$\frac{\mathrm{d}T(y_{\sigma m}(\beta))}{\mathrm{d}y_\sigma} = \beta - \sigma^2 r_\sigma(y_{\sigma m}(\beta)). \tag{27}$$

Differentiate with respect to β to get, after some manipulations and use of (26),

$$\frac{\mathrm{d}y_{\sigma m}(\beta)}{\mathrm{d}\beta} = \left(-A(\beta)\beta^{3/2} + \sigma^2 r'_\sigma(y_{\sigma m}(\beta))\right)^{-1}. \tag{28}$$

In principle, if $A(\beta)$ is known, (28) can be solved to give $y_{\sigma m}(\beta)$, the desired location, as a function of β, with an integration constant C. If A is known only in order of magnitude, this procedure will still provide $y_{\sigma m}(\beta)$ in order of magnitude.

To go further, the relation can be inverted to get β as a function of $y_{\sigma m}(\beta)$ and C. Next, one integrates (27) to get $T(y_\sigma)$ (with a second integration constant). Finally, integrate (18) twice to get $\Psi(y_\sigma)$ (approximately), and hence Φ from (15).

5.3. Conditions for logarithmic-like temperature profiles

It has long been recognized that the mean temperature profile (when Pe_τ is moderate or large) exhibits a logarithmic-like section [3,6]. The analysis now focuses on the conditions under which such a profile will be realized. In this regard, the simplest case is when $A(\beta)$ is constant and σ is so small that the $O(\sigma^2)$ terms in (28), (27) and (18) may be neglected. For this case, straightforward calculations show that $\Phi = C_1\sigma^2\ln(y_\sigma + C_2)$, and hence from (17) a similar logarithmic-like function of η.

But when can one expect $A(\beta)$ to be constant (or almost constant)? A similarity argument, as in [13,12] calls for the approximate constancy of $A(\beta)$ in the interior of the scaling layer hierarchy, and the same argument also applies here. Besides indicating conditions under which the temperature profile is expected to be logarithmic-like, the converse applies as well: if A is not constant, or the terms in σ^2 cannot reasonably be neglected, then the profile will not be logarithmic-like.

In this latter connection, it would be of interest to know when the term $\sigma^2 r'(y_{\sigma m}(\beta))$ in (28) may be neglected. For this, one might assume that r approaches its maximum at the centerline logarithmically (approximately), and r' decays like $\frac{1}{y_\sigma}$. Therefore that term might be negligible in comparison with the other term at locations y_σ where $\sigma^2(y_\sigma)^{-1} \ll \beta^{3/2}$. For example, this would be true for all $y_\sigma \gg 1$ if $\beta \geqslant \sigma^{4/3}$. Resolution of such details holds considerable promise in establishing the detailed circumstances under which the similarity between the temperature and velocity fields can be expected to exist.

5.4. Characteristic lengths, as they depend on distance from the wall

In this section, the small parameter σ^2 in (28) will be neglected. Let $\ell(\beta)$ denote the characteristic length in the layer L^θ_β, which will also be the order of magnitude of the width of that layer. From (24), one sees that

$$\ell(\beta) = O(\beta^{-1/2}), \tag{29}$$

and from (28), $\frac{dy_{\sigma m}}{d\beta} = -O(\beta^{-3/2})$ $(\beta \to 0)$ and integrating in view of (29), $y_{\sigma m} = O\ell$), i.e.

$$\ell(y_\sigma) = O(y_\sigma), \tag{30}$$

where now y_σ is a general location in the channel, and $\ell(y_\sigma)$ is the characteristic length of the profiles of Ψ and T at the location y_σ. These relations are asymptotic ones as $\beta \to 0$; this means that the location y_σ must correspond to a parameter β which is sufficiently small. Now interpret (30) in terms of the outer variable $\eta = \sigma^2 y_\sigma$ (from (17)). Both ℓ and y_σ are to be scaled in terms of η. That means that both are to be multiplied by σ^2. Eq. (30) remains invariant, and one obtains

$$\ell(\eta) = O(\eta). \tag{31}$$

Again, this relation holds for places η in the channel where T^β is maximal and $\beta \ll 1$. These place can be seen to be close to the wall. In words, what is revealed is that the characteristic length ℓ is asymptotically proportional to the outer distance η from the wall, for small η.

6. Discussion

Fully developed thermal transport through a wall-bounded turbulent flow with constant heat flux supplied at the wall was investigated via scaling considerations in coordination with observations based on DNS data. The present results provide a description of the scaling behaviors of the temperature and turbulent heat transfer profiles that is remarkably complete, considering that the point of departure is the averaged, therefore underdetermined, version of the thermal energy balance equation.

Although the thermal problem has many features formally in common with the classical fluid dynamical problem of steady turbulent flow through a channel, its additional independent parameter Pr brings an extra degree of uncertainty, as well as allowing for distinct phenomena. For example, the results of Fig. 2 clearly reveal that for $Pe_\tau \ll 1$ the molecular diffusion heat flux dominates over the turbulent counterpart over the entire channel. An analogous situation cannot exist in the momentum field. Despite such differences, a clear qualitative picture emerges when one takes into account certain clear monotonic dependencies on the parameter, Pe_τ, as seen in DNS data. In particular, the existence of a continuum of layers, a hallmark of classical turbulent flow through a channel, is also seen here for large Prandtl numbers. As a result, the existence, or nonexistence, of logarithmic-type profiles is clarified. Among other things, the monotone variation of the peak in the turbulent thermal flux with Pe_τ, known empirically, is predicted by the present framework.

A theme running through the present analysis is that considerable prior reasoning and certain conclusions regarding the analogous pure fluid dynamical problem can be taken over and used, with some modifications, in the present context. In doing so, the principal small parameter $\epsilon = (\delta^+)^{-1/2}$ in the former problem is replaced by the parameter σ in the latter, representing the (square root of the) deviation of the scaled centerline temperature from the wall temperature, as it depends on Pe_τ. This gives rise to the temperature scaling in (7); it is distinct from the one traditionally employed. Lastly, as with the velocity profile, direct analysis of the unintegrated form of the relevant governing equation reveals that the origin of a logarithmic temperature profile is independent of the classical inner/outer overlap ideas [7,20]. In this regard it is worth noting that, instead, the mathematical structure revealed herein provides theoretical justification for the classical distance from the wall scalings often hypothesized on physical grounds. Thus, justification comes about through the property that each patch L^θ_β of the scaling hierarchy has its width and characteristic length asymptotically proportional to the distance from the wall.

Acknowledgments

This work was supported by the US Department of Energy through the *Center for the Simulation of Accidental Fires and Explosions* under Grant W-7405-ENG-48, and the National Science Foundation under Grant CTS-0120061 (grant monitor, M. Plesniak).

References

[1] F.P. Incropera, D.P. DeWitt, Introduction to Heat Transfer, first ed., John Wiley & Sons, 1985.
[2] W.M. Kays, M. Crawford, Convective Heat and Mass Transfer, third ed., McGraw-Hill Education, 1993.
[3] B.A. Kader, A.M. Yaglom, Heat and mass transfer laws for fully turbulent wall flows, Int. J. Heat Mass Transfer 15 (1972) 2329–2351.
[4] Z. Warhaft, Passive scalar in turbulent flow, Annu. Rev. Fluid Mech. 32 (2000) 203–240.
[5] A.S. Monin, A.M. Yaglom, Statistical Fluid Mechanics, first ed., MIT Press, Cambridge, Massachusetts, 1971.
[6] B.A. Kader, Temperature and concentration profiles in fully turbulent boundary layers, Int. J. Heat Mass Transfer 24 (1981) 1541–1544.
[7] A.M. Yaglom, Similarity laws for constant-pressure and pressure-gradient turbulent wall flows, Annu. Rev. Fluid Mech. 11 (1979) 505–540.
[8] S.W. Churchill, C. Chan, Theoretically based correlating equations for the local characteristics of fully developed flow in round tubes and between parallel plates, Ind. Eng. Chem. Res. 34 (1995) 1332–1341.
[9] S.W. Churchill, New simplified models and formulations for turbulent flow and convection, AIChE J. 42 (1997) 1125–1140.

[10] S.W. Churchill, Turbulent flow and convection: the prediction of turbulent flow and convection in a round tube, Adv. Heat Transfer 34 (2001) 255–361.
[11] T. Wei, P. Fife, J. Klewicki, P. McMurtry, Properties of the mean momentum balance in turbulent boundary layer, pipe and channel flows, J. Fluid Mech. 522 (2005) 303–327.
[12] P. Fife, J. Klewicki, P. McMurtry, T. Wei, Multiscaling in the presence of indeterminacy: wall-induced turbulence. Multiscale Modeling Simul., in press.
[13] P. Fife, T. Wei, J. Klewicki, P. McMurtry, Stress gradient balance layers and scale hierarchies in wall-bounded turbulent flows, J. Fluid Mech. 532 (2005) 165–189.
[14] J. Klewicki, P. McMurtry, P. Fife, T. Wei, A physical model of the turbulent boundary layer consonant with the structure of the mean momentum balance, in: 15th Australasian Fluid Mechanics Conference, The University of Sydney, Sydney, Australia, 2004.
[15] T. Wei, P. McMurtry, J. Klewicki, P. Fife, Meso scaling of Reynolds shear stress in turbulent channel and pipe flows, AIAA J., in press.
[16] A. Perry, W.H. Schofield, Mean velocity and shear stress distributions in turbulent boundary layers, Phys. Fluids 16 (1973) 2068–2074.
[17] L.D. Landau, E.M. Lifshitz, Fluid Mechanics, first ed., Pergamon Press, London, 1959.
[18] H. Kawamura, H. Abe, K. Shingai, DNS of turbulence and heat transport in a channel flow with different Reynolds and Prandtl numbers and boundary conditions, in: Turbulence, Heat and Mass Transfer 3 (Proc. of the 3rd International Symposium on Turbulence, Heat and Mass Transfer), Aichi Shuppan, Japan, 2000, pp. 15–32.
[19] N. Kasagi, Y. Tomita, A. Kuroda, Direct numerical simulation of the passive scalar field in a two-dimensional turbulent channel flow, in: Proc. of 3rd ASME/JSME Thermal Engineering Joint Conference, Reno, 1991, pp. 175–182.
[20] C.B. Millikan, A critical discussion of turbulent flows in channel and circular tubes, in: J.P. Den Hartog, H. Peters (Eds.), Proc. 5th Int. Congr. Applied Mechanics, New York, 1938, Wiley, New York, 1938.